

## Detection and molecular cloning of *CYP74Q1* gene: Identification of *Ranunculus acris* leaf divinyl ether synthase

Q1 Svetlana S. Gorina, Yana Y. Toporkova, Lucia S. Mukhtarova, Ivan R. Chechetkin, Bulat I. Khairutdinov,  
4 Yuri V. Gogolev, Alexander N. Grechkin\*

5 Kazan Institute of Biochemistry and Biophysics, Russian Academy of Sciences, P.O. Box 30, 420111 Kazan, Russia

### ARTICLE INFO

#### Article history:

7 Received 13 March 2014

8 Received in revised form 10 May 2014

9 Accepted 16 May 2014

10 Available online xxxx

#### Keywords:

12 Divinyl ether synthase

13 Molecular cloning

14 CYP74Q1

15 P450

16 Oxylipins

17 Meadow buttercup (*Ranunculus acris* L.)

### ABSTRACT

Enzymes of the CYP74 family, including the divinyl ether synthase (DES), play important roles in plant cell sig- 19  
nalling and defence. The potent DES activities have been detected before in the leaves of the meadow buttercup 20  
(*Ranunculus acris* L.) and few other Ranunculaceae species. The nature of these DESs and their genes remained 21  
unrevealed. The PCR with degenerate primers enabled to detect the transcript of unknown P450 gene assigned 22  
as *CYP74Q1*. Besides, two more *CYP74Q1* isoforms with minimal sequence variations have been found. The full 23  
length recombinant CYP74Q1 protein was expressed in *Escherichia coli*. The preferred substrates of this enzyme 24  
are the 13-hydroperoxides of  $\alpha$ -linolenic and linoleic acids, which are converted to the divinyl ether oxylipins 25  
( $\omega$ 5Z)-etherolenic acid, (9Z,11E)-12-[(1'Z,3'Z)-hexadienyloxy]-9,11-dodecadienoic acid, and ( $\omega$ 5Z)-etheroleic 26  
acid, (9Z,11E)-12-[(1'Z)-hexenyloxy]-9,11-dodecadienoic acid, respectively, as revealed by the data of mass 27  
spectrometry, NMR and UV spectroscopy. Thus, CYP74Q1 protein was identified as the *R. acris* DES (RaDES), a 28  
novel DES type and the opening member of new CYP74Q subfamily. 29

© 2014 Published by Elsevier B.V.

### 1. Introduction

The oxidative metabolism of polyenoic fatty acids through the 36  
lipoxygenase pathway is a source of numerous oxylipins, which play im- 37  
portant roles in regulation of plant growth and development, cell signal- 38  
ling and defence [1,2]. Metabolism of fatty acid hydroperoxides and 39  
thus the diversity of oxylipins largely depend on the enzymes of CYP74 40  
family [1,2]. These are allene oxide synthase (AOS), hydroperoxide lyase 41  
(HPL) and divinyl ether synthase (DES) [1–4]. Hitherto the CYP74s were 42  
known only as the constituents of plant species. New CYP74 genes and 43  
enzymes have been detected recently in some proteobacteria and metazoan 44  
species [5]. Thus, the CYP74 family has been extended to the 45  
CYP74 clan [6], which includes new bacterial and metazoan members. A 46  
novel CYP74 enzyme, the epoxy alcohol synthase, has been detected 47  
recently in the lancelet *Branchiostoma floridae* [5]. 48

DESs have been detected in several flowering plant species [7–15]. 49  
Moreover, the divinyl ethers have been detected in brown alga *Laminaria* 50

*sinclairii* [16] and red alga *Polyneura latissima* [17], although no CYP74 51  
genes have been detected in algae yet [7]. DES genes of Solanaceae species 52  
(CYP74D) [18–20], garlic (CYP74H1) [21], and flax (CYP74B16) [22] have 53  
been cloned, and the properties of these recombinant DESs have been 54  
characterized. All other described DES activities have been detected in 55  
plant tissues, but the corresponding genes and proteins have not yet 56  
been detected, sequenced and cloned. Divinyl ethers play the defensive 57  
and antimicrobial role in plants [23–27]. 58

Majority of DESs are present in non-green plant tissues, e.g. potato 59  
tubers, tomato roots, and garlic bulbs [7]. There are only two known 60  
DESs present in plant leaves. These are flax [13,22] and Ranunculaceae 61  
[10–12] DESs. Flax DES has been recently cloned and identified as 62  
CYP74B16 [22], an unprecedented 13-DES member of the CYP74B sub- 63  
family, while all other CYP74B members are 13-HPLs [7]. The nature of 64  
Ranunculaceae DESs remains uncovered. This prompted us to look for 65  
the CYP74 transcripts in *Ranunculus acris* leaves. Using the degenerate 66  
primers, we succeeded to detect an unknown CYP74 transcript. The pres- 67  
ent paper reports the cloning of corresponding full length cDNA and iden- 68  
tification of the recombinant protein as *R. acris* DES (RaDES), CYP74Q1. 69

### 2. Materials and methods

#### 2.1. Materials

The aerial parts of wild *R. acris* plants were collected near the lake 72  
Sredny Kaban (Kazan) in Summer seasons 2012 and 2013. Linoleic 73  
and  $\alpha$ -linolenic acids, as well as the soybean lipoxygenase type V, 74

Abbreviations: DES, divinyl ether synthase; RaDES, *Ranunculus acris* divinyl ether 75  
synthase; HPL, hydroperoxide lyase; AOS, allene oxide synthase; 13(S)-HPOT, 76  
(9Z,11E,13S,15Z)-13-hydroperoxyoctadecatrienoic acid; 13(S)-HPOD, (9Z,11E,13S)-13- 77  
hydroperoxyoctadecadienoic acid; 9(S)-HPOD, (9S,10E,12Z)-9-hydroperoxyoctadecadienoic 78  
acid; IMAC, immobilized metal affinity chromatography (IMAC); TMS, trimethylsilyl; GC- 79  
MS, gas chromatography-mass spectrometry; ECL, equivalent chain lengths; ORF, open read- 80  
ing frame; IHCD, I-helix central domain, the catalytically important six amino acid domain in 81  
the centre of P450 I-helix

\* Corresponding author. Tel.: +7 843 292 75 35; fax: +7 843 292 73 47.

E-mail address: [grechkin@mail.knc.ru](mailto:grechkin@mail.knc.ru) (A.N. Grechkin).

**Table 1**  
 Degenerate oligonucleotide primers used in PCR for the detection of the CYP74 genes transcripts in *Ranunculus acris* leaves transcriptome.

Name	Primer sequence 5' to 3'	T <sub>m</sub> , °C
RaF1	gA(A/g)AAg(C/g)ACAAgAgCAC(g/C)gT(g/T)TTC	58.2/60.2
RaR1	CA(T/A)Ag(A/C)A(g/A)CTC(C/g/A)CCTTCTTg	43.6/57.9
RaF2	CT(T/C)gT(T/C)gg(T/C/g)gA(T/C)TTCATgCC	50.3/59.0
RaR2	ggCATgAA(g/A)TC(C/g/A)CC(g/A)AC(g/A)Ag	50.3/60.2

were purchased from Sigma. Adams's catalyst and silylating reagents were purchased from Fluka (Buchs, Switzerland). (9S,10E,12Z)-9-Hydroperoxy-10,12-octadecadienoic acid (9-HPOD) was prepared by incubation of linoleic acid with tomato fruit lipoxygenase at 0 °C, pH 6.0, under continuous oxygen bubbling. (9Z,11E,13S,15Z)-13-Hydroperoxy-9,11,15-octadecatrienoic (13-HPOT) and (9Z,11E,13S)-13-hydroperoxy-9,11-octadecadienoic (13-HPOD) acids were obtained by incubation of α-linolenic and linoleic acids, respectively, with the soybean lipoxygenase type V. All hydroperoxides were purified by normal phase HPLC.

2.2. Bioinformatic methods for the CYP74 structure analysis

The primary structures of the CYP74s were aligned using NCBI and PlantGDB BLAST searches, as well as the Clustal Omega tool. The phylogenetic tree of selected CYP74 clan members was built with the Clustal Omega and the TreeView software.

2.3. Expression and purification of recombinant enzymes

The open reading frame (ORF) of gene *RaDES* has been cloned into the vector pET32-Ek/LIC (Novagen, USA) to yield the target recombinant protein with His-tags at N- and C-termini. The resulting construction was transformed into *Escherichia coli* host strain Rosetta-gami(DE3)pLysS B. The expression of recombinant gene in *E. coli* cells was induced by adding 0.5 mM isopropyl-β-D-1-thiogalactopyranoside to the medium. His-

tagged recombinant protein was purified by immobilized metal affinity chromatography (IMAC) using Bio-Scale Mini Profinity IMAC cartridge and BioLogic LP chromatographic system (Bio-Rad, USA) [22]. The homogeneity of purified protein was confirmed by SDS-PAGE. Protein concentration was estimated as described before [22]. The enzyme activity was measured with Lambda 25 spectrophotometer (Perkin-Elmer, USA) by the decrease of fatty acid hydroperoxides absorbance at 234 nm [22].

2.4. Incubations of recombinant enzyme with fatty acid hydroperoxides

The recombinant enzyme (10 μg) was incubated with 100 μg of fatty acid hydroperoxide in Na-phosphate buffer (2 ml), pH 7.0, 4 °C, for 15 min. The products were extracted, purified with solid phase cartridges, methylated with diazomethane and trimethylsilylated as described before [22], followed by GC-MS analysis. When specified, the products were reduced with NaBH<sub>4</sub> and hydrogenated over PtO<sub>2</sub>, then methylated and trimethylsilylated. Products (without or with the preliminary hydrogenation and reduction) were analyzed as Me esters/TMS derivatives (Me/TMS) by GC-MS as described before [22].

2.5. Kinetic studies

The enzymatic activity of the purified recombinant RaDES was determined by monitoring the increase of the signal at 250 nm or 267 nm (for 13-HPOD and 13-HPOT, respectively) in a Varian 50 Bio UV-VIS spectrophotometer with substrate concentrations ranging from 5 to 210 μM. The analyses were performed in 0.6 ml of 0.05 M Na phosphate buffer (pH 7.5) at 25 °C. The initial linear regions of the kinetic curves were used to calculate the rates. The amounts of products, namely (ω5Z)-etherolenic and (ω5Z)-etheroleic acids, formed were estimated using the molar extinction coefficients 41,200 M<sup>-1</sup> cm<sup>-1</sup> and 25,700 M<sup>-1</sup> cm<sup>-1</sup>, respectively. The latter value is the difference between the molar extinction coefficients 32,100 M<sup>-1</sup> cm<sup>-1</sup> and 6400 M<sup>-1</sup> cm<sup>-1</sup> for (ω5Z)-etheroleic acid and 13-HPOD at 250 nm, respectively. Kinetic parameters were calculated by fitting the datasets to a one-site saturation model for simple

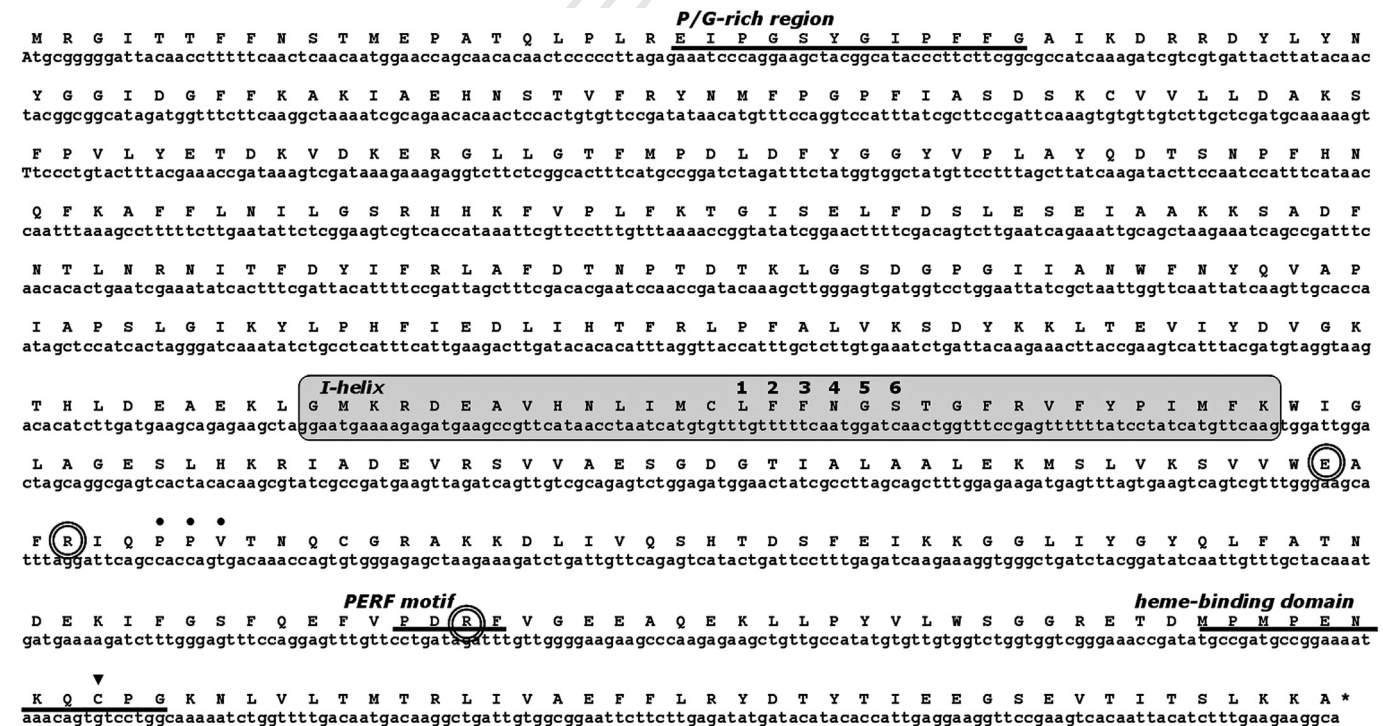


Fig. 1. Nucleotide and the deduced amino acid sequences of the target *Ranunculus acris* CYP74Q1 cDNA. Conservative domains are marked as follows: the I-helix is outlined with gray rounded rectangle; the IHCD domain is numbered 1-6; ERR-triad is outlined with double circles; P/G-rich region, PERF-motif and haem-binding domain are underlined with bold lines; black triangle shows the position of the conserved cysteinyl haem ligand.

			IHCD
RaDES	CYP74Q1	(275)	GMKRDEAVHNLIMCLFENGSTGFRVFPYIMFKWI
AsDES	CYP74H1	(260)	GLSREEAITHHLIFTWAINAYLCIRTCMLRIFKWI
ZmHPL	CYP74F2	(281)	GIGKKDAINNILFVLGFNAFGGFSVFLPFLVAKV
OsHPL1	CYP74E2	(284)	GIPRDELLHNLVVFVAVENAYGGFKIFLPHIVKWL
StDES	CYP74D2	(266)	GIKREEAVQNILFVLGINMFAAGLNAFSPHIFRFV
LeDES	CYP74D1	(266)	GIKREEAVQNILFVLGINMFAAGLNAFSPHIFRFV
PdHPL	CYP74C5	(271)	GLSREEACHNLLFVAGFNAGGGMKLLFEALIKWV
CmHPL	CYP74C2	(267)	GIDREKACHNLLVFLAGFNAYGGMKVLFPDLLKVV
StAOS3	CYP74C10	(280)	GVKREEACHNFIFLAGFNAYGGMKVVFFPSLIKWI
LeAOS3	CYP74C3	(280)	GVKRDEACHNFVFLAGFNAYGGLKVVFFPSLIKWI
PgHPL	CYP74B5	(289)	GLTHQEAITHNLLFIFLGFNAFGGFSIFLPTLLSNL
CaHPL	CYP74B1	(275)	QLTEQEAITHNLLFIFLGFNAFGGFTIFLPTLLGNL
StAOS2	CYP74A6v1	(209)	GISKEEACHNLLFATCFNSFGGMKIFFFNMMKSI
LeAOS1	CYP74A1	(321)	GISREEACHNLLFATCFNSFGGIKIFFFNMLKWI
Consensus			GIKREEACHNLLFVLAGFNAGGFK+FFP+L+KWI

**Fig. 2.** The multiple alignments of I-helix domains of CYP74Q1 and selected enzymes of different CYP74 subfamilies. The IHCD domain is outlined with rectangle and signed on the top. The alignments were built with Clustal Omega tool.

127 ligand binding using the SigmaPlot 11 software (Systat Software Inc.,  
128 USA). Five independent experiments were performed for each specified  
129 variant. The mean values and standard deviations are given.

### 130 2.6. Methods of spectral analyses

131 The UV spectra of products were scanned during the incubations of  
132 the recombinant RaDES with fatty acid hydroperoxides with Varian  
133 Cary 50 spectrophotometer. The UV spectra of purified enzyme products  
134 were recorded with the same instrument. Alternatively, the UV spectra of  
135 products were recorded on-line during the HPLC separations using an  
136 SPD-M20A diode array detector (Shimadzu). Products were analyzed as  
137 methyl esters or methyl esters/TMS derivatives by GC-MS as described  
138 before [9]. The GC-MS analyses were performed using a Shimadzu  
139 QP5050A mass spectrometer connected to Shimadzu GC-17A gas chro-  
140 matograph equipped with a Supelco MDN-5S (5% phenyl 95% methyl-  
141 polysiloxane) fused capillary column (length, 30 m; ID 0.25 mm; film  
142 thickness, 0.25  $\mu\text{m}$ ). Helium at a flow rate of 30 cm/s was used as the

143 carrier gas. Injections were made in the split mode using an initial column  
144 temperature of 120 °C, injector temperature 230 °C. The column temper-  
145 ature was raised at 10 °C/min until 240 °C. The electron impact ionization  
146 (70 eV) has been used. The equivalent chain lengths (ECL) values were es-  
147 timated as described before [28]. The  $^1\text{H}$  NMR and 2D-COSY spectra were  
148 recorded with a Bruker Avance III 600 instrument (600 MHz,  $[\text{D}_6]\text{benzene}$ ,  
149 296 K).

## 150 3. Results

### 151 3.1. Design of degenerate primers for CYP74 transcript detection

152 The *R. acris* genome has not been sequenced yet. Only a very lim-  
153 ited number of *R. acris* gene sequences is published, among them  
154 there are no P450 genes. No CYP74 ESTs of Ranunculaceae are cur-  
155 rently present in the genomic databases. Thus, there was no genomic  
156 background that could facilitate the identification of *RaDES* gene.  
157 That is why an approach with degenerate primers was used in the  
158 present work. Recently we succeeded to detect and clone the before  
159 unknown flax CYP74B16 gene using degenerate primers although  
160 flax genome was not sequenced at that time [22]. In the present  
161 work, we used the same approach to detect the CYP74 mRNAs in  
162 *R. acris* leaf transcriptome. To design the degenerate primers, we an-  
163 alyzed the alignments of CYP74 amino acid sequences to find the  
164 most conserved domains.

165 The first step in the design of degenerate primers was a search  
166 for conservative motifs in sequences of the different plant CYP74s.  
167 Primer regions were chosen so that the resulting amplicons would  
168 contain the I-helix central domain (IHCD [29], which is referred to  
169 “the oxygen-binding domain” in the case of monooxygenases).  
170 The sequences of all constructed degenerate primers used for the  
171 PCR search of CYP74 transcripts are listed in Table 1.

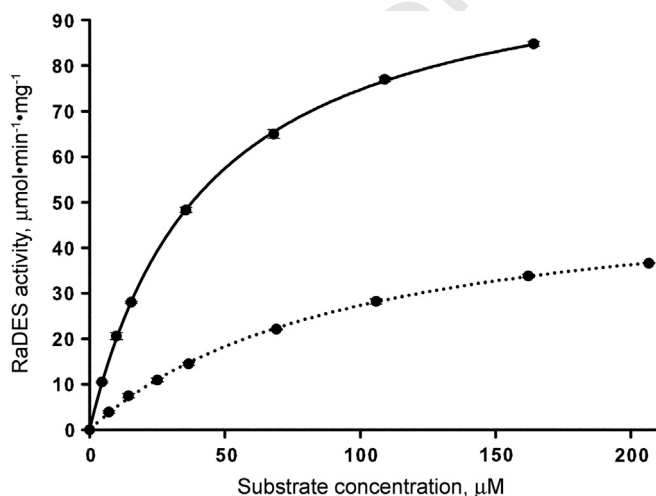


**Fig. 3.** Substrate saturation curves for the recombinant RaDES. Kinetic data were recorded with double beam spectrophotometer as described in Materials and methods. The quantitative kinetic parameters for the data representing conversions of 13-HPOT (solid line) and 13-HPOD (dotted line) were fitted to a one-site saturation model for simple ligand binding using the SigmaPlot 11 software as described in Materials and methods.

**Table 2**

Kinetic parameters and substrate specificity of the recombinant RaDES.

Substrate	$k_{cat}$ ( $\text{s}^{-1}$ )	$K_M$ ( $\mu\text{M}$ )	$k_{cat}/K_M$ ( $\mu\text{M}^{-1} \text{s}^{-1}$ )	Substrate specificity, % 13(S)-HPOT
13-HPOT	$134.0 \pm 1.4$	$43.1 \pm 1.1$	3.11	100
13-HPOD	$67.7 \pm 1.1$	$97.6 \pm 3.5$	0.69	22
9-HPOT	–	–	–	0 <sup>a</sup>
9-HPOD	–	–	–	0 <sup>a</sup>

<sup>a</sup> No divinyl ethers have been detected upon the incubations with 9-HPOT and 9-HPOD.

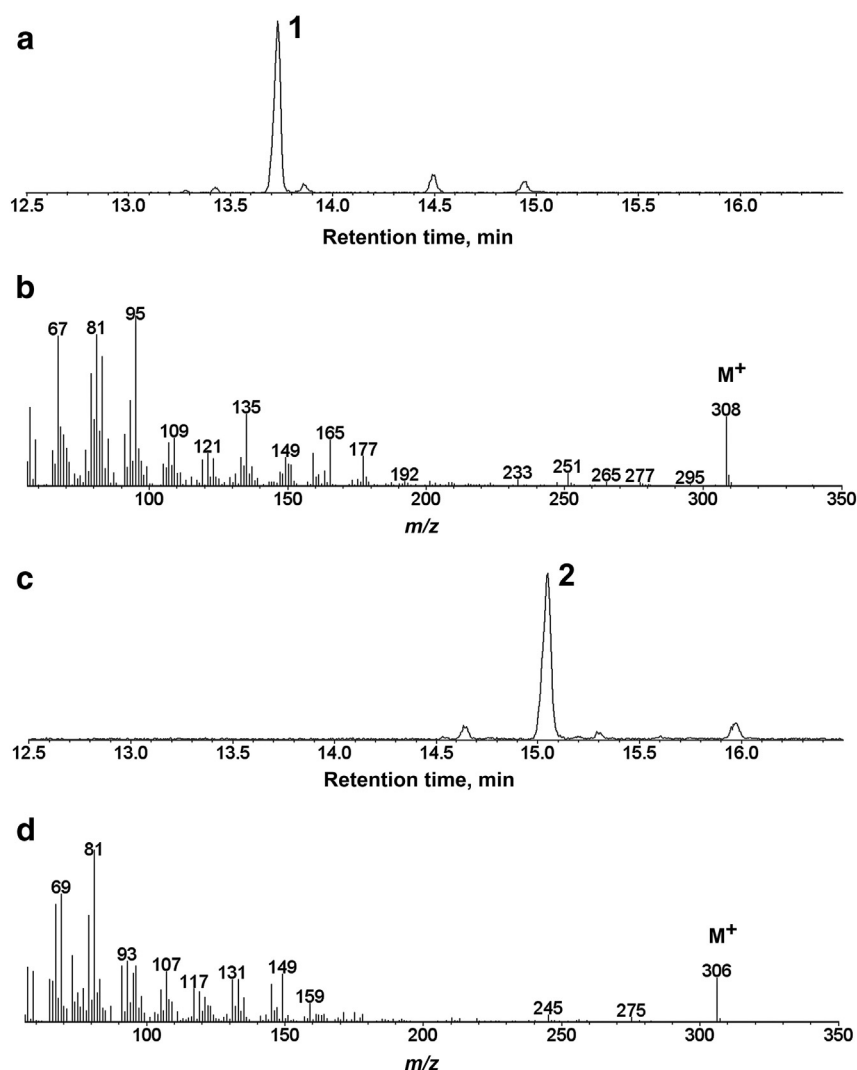


**Fig. 4.** The GC-MS analyses of RaDES products. (a) The GC-MS chromatogram of products (Me/TMS) of 13-HPOT incubation with CYP74Q1. (b) The mass spectrum for product 1. (c) The GC-MS chromatogram of products (Me/TMS) of 13-HPOD incubation with CYP74Q1. (d) The mass spectrum for product 2.

### 3.2. Detection and cloning of CYP74Q1 gene

The total RNA was isolated from the leaves of *R. acris* plants. The cDNA obtained after the reverse transcription was used as the template for PCR with the constructed primers (Table 1). The resulting ca. 1000 bp products obtained in PCR with primers RaF1-RaR1 were initially cloned into pGEM-T vector (Promega, USA) and subjected to DNA sequencing to verify the presence of any CYP74 fragments. The detected partial CYP74 sequences were used to construct the gene-specific primers (supplementary Table S1, supplementary Fig. S1) for the detection of 3' and 5' cDNA ends by RACE method. 3' and 5' cDNA ends were obtained in reaction with "Mint RACE cDNA amplification set" (Evrogen, Russia) in three serial PCRs using gene-specific primers and universal Step-out primer mix1, Step-out primer mix2, Step-out primer mix3 (supplementary Fig. S1) according to the manufacturer's protocol. Thus, the novel full length CYP74 gene was sequenced and cloned. Its nucleotide and deduced amino acid sequences are presented in Fig. 1. The screening of cDNA library revealed two additional isoforms possessing some minor sequence variations as shown in supplementary Fig. S2.

The ORF (Fig. 1) of isoform 1 consisted of 1449 nucleotides and encoded 483 amino acid polypeptide (Fig. 1). The sequence alignments of isoform 1 demonstrated that the novel *R. acris* CYP74 protein does

not belong to any known CYP74 subfamily. Thus, this is the first representative of novel subfamily CYP74Q. The name CYP74Q1 has been assigned to this new sequence [Professor David R. Nelson, personal communication]. The multiple alignment of CYP74Q1 (I-helix domain) and other CYP74s is illustrated in Fig. 2. The deduced CYP74Q1 amino acid sequence does not belong to any previously known CYP74 subfamily. It has 52% identity to CmHPL (CYP74C2), 51% to putative AOS (CYP74C9) of *Petunia integrifolia* subsp. *inflata*, 49% to LeDES (CYP74D1) and 49% to HbAOS (CYP74A9).

### 3.3. Substrate specificity and kinetics of the recombinant CYP74Q1

Recombinant CYP74Q1 (RaDES) efficiently utilized 13-HPOT and 13-HPOD (Fig. 3). At the same time, the enzyme was quite inactive towards 9-HPOD and 9-HPOT in full agreement with the literature data [11]. RaDES exhibited the hyperbolic kinetic profiles for both 13-HPOT and 13-HPOD conversions (Fig. 3). The  $K_M$  values (Table 2) demonstrated that RaDES affinity for 13-HPOT was over twice higher than for 13-HPOD. The estimated turnover rate ( $k_{cat}$ ) of 13-HPOT was about twice higher than that of 13-HPOD (Table 2). As judged by specificity constant ( $k_{cat}/K_M$ ) values (Table 2), 13-HPOT was the preferential substrate for RaDES.

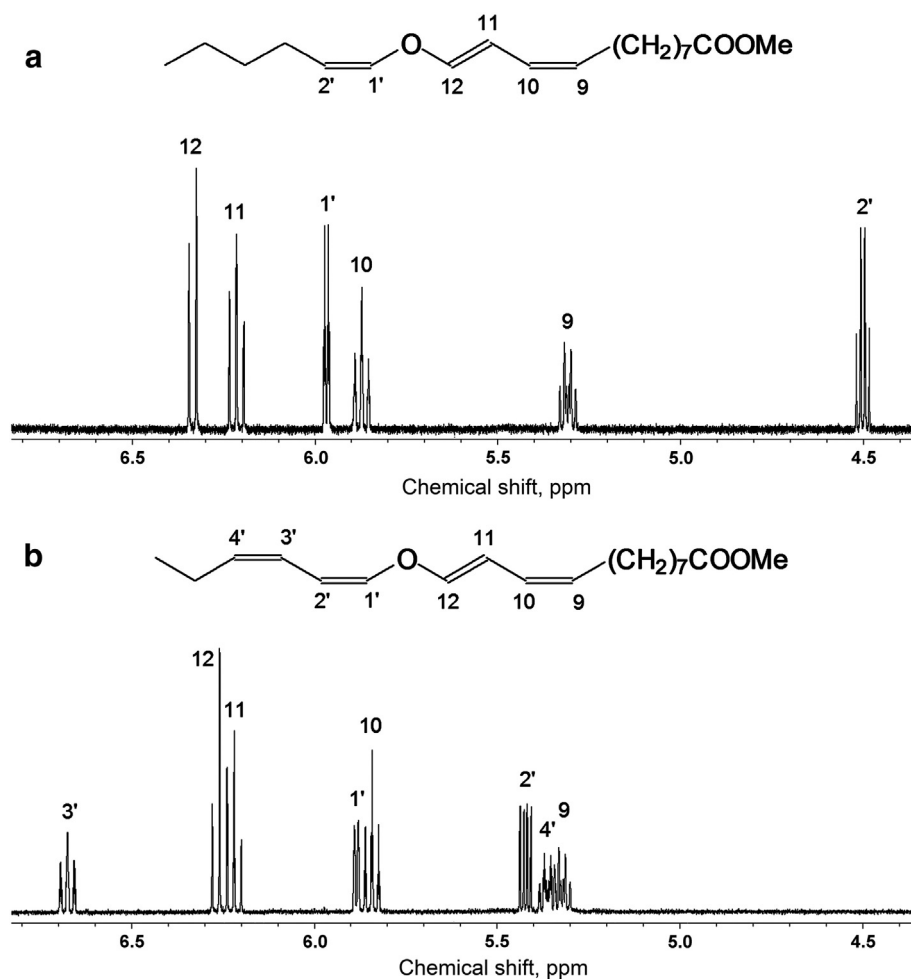


**Fig. 5.** The olefinic regions of  $^1\text{H-NMR}$  spectra (600 MHz,  $[\text{D}_6]\text{benzene}$ , 296 K) of products **1** (a) and **2** (b). Methine position number is specified at the top of each multiplet. Insets, the structural formulae of products **1** and **2** with numbered positions of olefinic protons.

#### 214 3.4. Identification of the recombinant CYP74Q1 as divinyl ether synthase

215 The GC-MS analyses of the products (Me/TMS) revealed a specific  
 216 conversion of 13-HPOD to product **1** (Fig. 4a). Its mass spectrum  
 217 (Fig. 4b) possessed  $\text{M}^+$  at  $m/z$  308 (21%),  $[\text{M} - \text{MeO}]^+$  at  $m/z$  277  
 218 (2%),  $[\text{M} - \text{Me}(\text{CH}_2)_3]^+$  at  $m/z$  251 (4%),  $m/z$  219 (3%),  $m/z$  177  
 219 (15%), and  $[\text{M} - (\text{CH}_2)_6\text{COOMe}]^+$  at  $m/z$  165 (19%). The spectral pat-  
 220 terns were identical to those of  $(\omega 5Z)$ -etheroleic acid [10]. The  
 221 equivalent chain length (ECL) value (19.05) of product **1** peak  
 222 corresponded to  $(\omega 5Z)$ -etheroleic acid. It is much smaller compared  
 223 to other geometric isomers of etheroleic acid, having the ECL values  
 224 above 19.5. To substantiate the structural identification including  
 225 the double bond geometry, we purified product **1** (Me ester) by  
 226 HPLC and recorded its  $^1\text{H-NMR}$  and 2D-COSY spectra (Fig. 5a  
 227 and supplementary Table S2). The data fully confirmed the identifi-  
 228 cation of product **1** as  $(\omega 5Z)$ -etheroleic acid, (9Z,11E)-12-[(1'Z)-  
 229 hexenyloxy]-9,11-dodecadienoic acid.

230 RaDES was most efficient towards 13-HPOT. 13-HPOT was quite  
 231 specifically converted to a single predominant product **2** (detected  
 232 as Me ester), as illustrated in Fig. 4c. Mass spectrum of compound **2**  
 233 (Fig. 4d) exhibited  $\text{M}^+$  at  $m/z$  306 (27%),  $[\text{M} - \text{Et}]^+$  at  $m/z$  277  
 234 (2%),  $[\text{M} - \text{MeO}]^+$  at  $m/z$  275 (2%),  $[277 - \text{MeOH}]^+$  at  $m/z$  245  
 235 (4%), and  $[\text{M} - (\text{CH}_2)_7\text{COOMe}]^+$  at  $m/z$  149 (25%). The spectrum  
 236 matched that of  $(\omega 5Z)$ -etherolenic acid. The ECL value 20.03 of  
 237 this peak also corresponded to that of  $(\omega 5Z)$ -etherolenic acid. It  
 238 should be noted that  $(\omega 5Z)$ -etherolenic and etherolenic acids  
 239 coelute during the GC separation on the nonpolar stationary

240 phases. Thus, to reveal the exact double bond geometry, the product  
 241 **2** (Me) was isolated and purified by RP-HPLC and NP-HPLC.  
 242 Then the  $^1\text{H-NMR}$  and 2D-COSY data (Fig. 5b and supplementary  
 243 Table S3) were recorded. These data unambiguously revealed the  
 244 structure of compound **2** as  $(\omega 5Z)$ -etherolenic acid, (9Z,11E)-12-  
 245 [(1'Z,3'Z)-hexadienyloxy]-9,11-dodecadienoic acid.

#### 246 4. Discussion

247 Ranunculaceae species (Ranunculales, basal Eudicots) are phylogeneti-  
 248 cally distant from other plants possessing DESs. Although DESs were  
 249 detected in tissues of few Ranunculaceae species [10–12], neither DES  
 250 proteins nor their genes have been sequenced and cloned. RaDES  
 251 (CYP74Q1) presents a new extension to the known diversity of DESs.  
 252 DESs of Solanaceae species belong to CYP74D subfamily, while garlic  
 253 (*Allium sativum* L.) DES is the only member of CYP74H subfamily. The recently  
 254 described flax enzyme LuDES (CYP74B16) is an unusual DES, belonging  
 255 to CYP74B subfamily [22]. All other known members of this subfamily are  
 256 13-HPLs. DESs of CYP74D subfamily, as well as DES of garlic, are expressed  
 257 in non-green plant organs [8]. In contrast, CYP74Q1 and CYP74B16 [22]  
 258 are expressed in the leaves of *R. acris* and flax, respectively. Both enzymes  
 259 preferentially utilize 13-hydroperoxides of linolenic and linoleic acids,  
 260 while 9-hydroperoxides are poor substrates. Despite these similarities,  
 261 CYP74Q1 and CYP74B16 are phylogenetically distant from each other.  
 262 They possess only 36% identity.

263 Various DESs differ in respect of substrate and product specificities.  
 264 The “leaf DESs” RaDES (CYP74Q1), as well as LuDES (CYP74B16), are

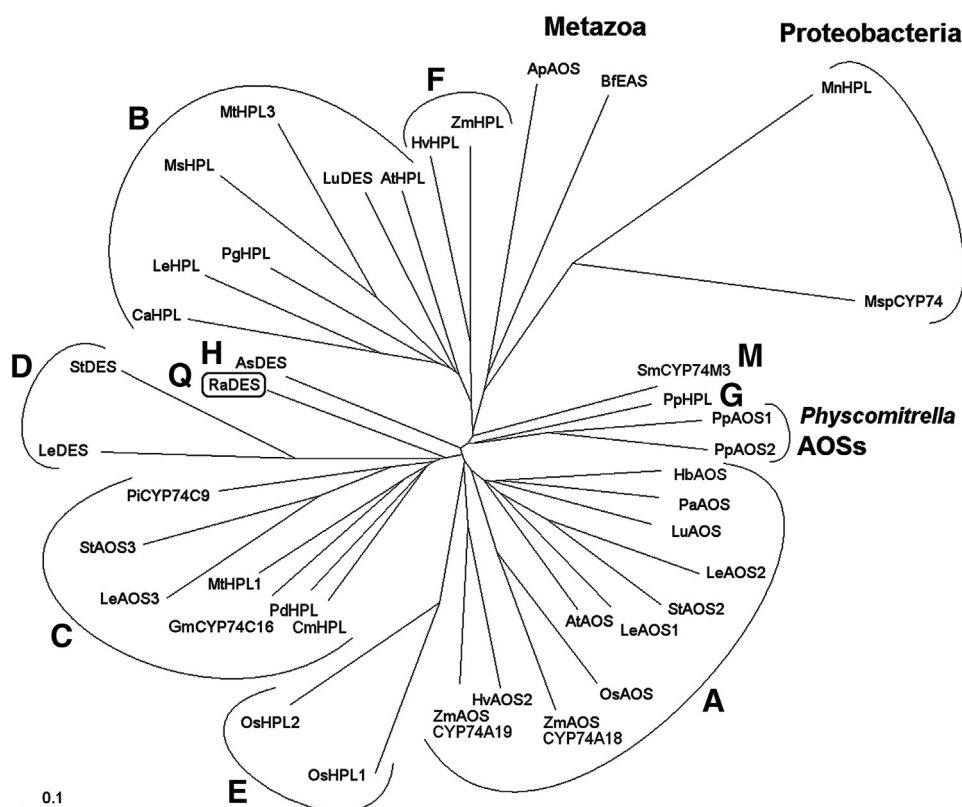


**Fig. 6.** The unrooted phylogenetic tree of CYP74 clan. Classified CYP74 subfamilies are marked with their letter designations (A, B, C etc.). Subfamilies consisting of more than one member are outlined with unclosed curves (semi-ellipses). RaDES (CYP74Q1) is outlined with rounded rectangle. CYP74s of flowering plants: As, *Allium sativum*; AsDES, GI:83414021; At, *Arabidopsis thaliana*; AtAOS, CYP74A1, GI:15239032; AtHPL, CYP74B2, GI:3822403; Ca, *Capsicum annuum*; CaHPL, CYP74B1, GI:1272340; Cm, *Cucumis melo*; CmHPL, CYP74C2, GI:14134199; Gm, *Glycine max*; GmCYP74C16, GI:100037482; Hb, *Hevea brasiliensis*; HbAOS, CYP74A9, GI:84028363; Hv, *Hordeum vulgare*, HvAOS2, GI:7452981; HvHPL, CYP74F3, GI:22265998; Le, *Lycopersicon esculentum*; LeAOS1, GI:7581989; LeAOS2, CYP74A2, GI:7677376; LeAOS3, CYP74C3, GI:25991603; LeHPL, GI:7677378; LeDES, GI:11991245; Lu, *Linum usitatissimum*; LuAOS, CYP74A1, GI:1352186; LuDES, CYP74B16, GI:310687282; Ms, *Medicago sativa*; MsHPL, GI:5830465; Mt, *Medicago truncatula*; MhHPL1, CYP74C12, GI:33504430; MhHPL3, CYP74B4, GI:63081244; Os, *Oryza sativa*; OsAOS, CYP74A4, GI:115455571; OsHPL1, CYP74E2, GI:115445057; OsHPL2, CYP74E1, GI:125538638; Pa, *Parthenium argentatum*; PaAOS, CYP74A1, GI:218511958; Pd, *Prunus dulcis*; PdHPL, CYP74C5, GI:33300600; Pg, *Psidium guajava*; PgHPL, CYP74B5, GI:13183137; Pi, *Petunia inflata*; PiCYP74C9, GI:85720841; Sm, *Selaginella moellendorffii*; SmCYP74M3, GI:9654395; St, *Solanum tuberosum*; StAOS2, GI:86769479; StAOS3, GI:56605358; StDES, CYP74D2, GI:12667099; Zm, *Zea mays*; ZmAOS, CYP74A18, GI:223947589; ZmAOS, CYP74A19, GI:223947589; ZmHPL, CYP74F2, GI:162462890. CYP74s of mosses: Pp, *Physcomitrella patens*; PpAOS1, CYP74A1, GI:22217985; PpAOS2, CYP74A8, GI:168014176; PpHPL, CYP74G1, GI:76057841. CYP74 clan members of proteobacteria: Mn, *Methylobacterium nodulans*; MnHPL, GI:220926268; Msp, *Methylobacterium* sp. 4-46; MspHPL (putative HPL), GI:170743950. CYP74 clan members of Metazoa: Ap, *Acropora palmata* (coral); ApAOS, GI:187948710; Bf, *B. floridae* (lancelet); BfEAS, GI:189312561. The tree was built with the Clustal Omega and the TreeView software using the alignments of full amino acid sequences of the above listed CYP74 clan members. The preliminary BLAST analyses of CYP74s were performed using the protein NCBI BLAST tool.

265 the specific 13-DESs. Their distinguishing feature is the production of  
 266 ( $\omega$ 5Z)-etherolenic and ( $\omega$ 5Z)-etheroleic acids. In contrast, the “classic”  
 267 DESs of Solanaceae (CYP74D) are 9-DESs and produce the colnelenic  
 268 and colnelenic acids. The garlic DES (CYP74H1) utilizes both 13- and 9-  
 269 hydroperoxides of linoleic and linolenic acids and produces either  
 270 etheroleic and etherolenic or colnelenic and colnelenic acids, respectively.  
 271 CYP74Q1 has 52% identity to CmHPL (CYP74C2), 51% to putative  
 272 AOS (CYP74C9) of *P. integrifolia* subsp. *inflata*, 49% to LeDES  
 273 (CYP74D1) and 49% to HbAOS (CYP74A9). Thus, CYP74Q is nearly  
 274 equally distant towards CYP74C, CYP74D and CYP74A subfamilies;  
 275 see the phylogenetic tree of CYP74 clan, Fig. 6. Interestingly, RaDES  
 276 (CYP74Q1), AsDES (CYP74H1) and CYP74D subfamily DESs are  
 277 grouped into a cluster on the phylogenetic tree (left side of tree,  
 278 Fig. 6).

279 It is worthwhile that plant evolution created a big diversity of dis-  
 280 tinct DES types. Known DESs belong to subfamilies CYP74B (LuDES,  
 281 CYP74B16), CYP74D (Solanaceae DESs), CYP74H (AsDES), CYP74M3  
 282 and CYP74Q (RaDES). DESs are not as widespread as AOSs and HPLs.  
 283 Some of the sequenced plant genomes like those of *Arabidopsis thaliana*  
 284 and *Oryza sativa* do not possess any DES gene. At the same time, it is too  
 285 early to make conclusions on the commonness of DES genes. The cur-  
 286 rent state of genomic knowledge is too incomplete. One can expect

287 that further progress will uncover many new DESs not only in Plant  
 288 Kingdom, but possibly also in some metazoans. The tree of CYP74 clan  
 289 continues to grow, and there are certainly still large gaps to be filled.

290 Regardless of the limited occurrence of DES genes, each separate DES  
 291 type has evidently been evolved from gene duplication and independ-  
 292 ent evolution targeted to the creation of DES catalysis. For instance,  
 293 the recently detected LuDES although belonging to CYP74B subfamily,  
 294 possesses only ca. 70% identity to the putative flax HPL (Lus10030029,  
 295 CYP74B). These two flax genes were evidently evolved through the  
 296 duplication and divergence. Indeed, the qualitative changes of CYP74  
 297 catalysis can occur due to site-directed mutagenesis. For instance, the  
 298 AOSs to HPLs [5,30] as well as DESs to AOSs [30] conversions have  
 299 been demonstrated.

#### Acknowledgements

300 This work was supported in part by 12-04-01140-a and 12-04-  
 301 97059-r from the Russian Foundation for Basic Research, a grant  
 302 from the Russian Academy of Sciences (program ‘Molecular and  
 303 Cell Biology’), a grant from program ‘Leading Scientific Schools’  
 304 and a grant MK-4886.2013.4 (Y.Y. Toporkova) of the President of  
 305 Russian Federation for Young Scientists. Mass spectral records by  
 306

307 Dr. Fakhima K. Mukhitova are gratefully acknowledged. We thank Profes-  
 308 sor David R. Nelson (Tennessee University) for the nomenclature discus-  
 309 sion and making the CYP74Q1 assignment.

### 310 Appendix A. Supplementary data

311 Supplementary data to this article can be found online at <http://dx.doi.org/10.1016/j.bbaliip.2014.05.005>.

### 313 References

- 314 [1] E. Blée, Phytooxylipins and plant defense reactions, *Prog. Lipid Res.* 37 (1998)  
 315 33–72.  
 316 [2] A.N. Grechkin, Recent developments in biochemistry of the plant lipoxygenase path-  
 317 way, *Prog. Lipid Res.* 37 (1998) 317–352.  
 318 [3] M. Stumpe, I. Feussner, Formation of oxylipins by CYP74 enzymes, *Phytochem. Rev.*  
 319 5 (2006) 347–357.  
 320 [4] R.K. Hughes, S. De Domenico, A. Santino, Plant cytochrome CYP74 family: biochemi-  
 321 cal features, endocellular localisation, activation mechanism in plant defence and  
 322 improvements for industrial applications, *ChemBioChem* 10 (2009) 1122–1133.  
 323 [5] D.-S. Lee, P. Nioche, M. Hamberg, C.S. Raman, Structural insights into the evolution-  
 324 ary paths of oxylipin biosynthesis enzymes, *Nature* 455 (2008) 363–370.  
 325 [6] D.R. Nelson, J.V. Goldstone, J.J. Stegeman, *Phil. Trans. R. Soc. B.* 368 (2013) 20120474.  
 326 [7] A.N. Grechkin, Hydroperoxide lyase and divinyl ether synthase, *Prostaglandins*  
 327 *Other Lipid Mediat.* 68–69 (2002) 457–470.  
 328 [8] A.N. Grechkin, F.N. Fazliev, L.S. Mukhtarova, The lipoxygenase pathway in garlic (*Allium*  
 329 *sativum* L.) bulbs: detection of the novel divinyl ether oxylipins, *FEBS Lett.* 371 (1995)  
 330 159–162.  
 331 [9] A.N. Grechkin, A.V. Ilyasov, M. Hamberg, On the mechanism of biosynthesis of divinyl  
 332 ether oxylipins by enzyme from garlic bulbs, *Eur. J. Biochem.* 245 (1997) 137–142.  
 333 [10] M. Hamberg, A pathway for biosynthesis of divinyl ether fatty acids in green leaves,  
 334 *Lipids* 33 (1998) 1061–1071.  
 335 [11] M. Hamberg, Biosynthesis of new divinyl ether oxylipins in *Ranunculus* plants, *Lipids* 37  
 336 (2002) 427–433.  
 337 [12] M. Hamberg, Isolation and structures of two divinyl ether fatty acids from *Clematis*  
 338 *vitalba*, *Lipids* 39 (2004) 565–569.  
 339 [13] I.R. Chechetkin, A. Blufard, M. Hamberg, A.N. Grechkin, A lipoxygenase-divinyl ether  
 340 synthase pathway in flax (*Linum usitatissimum* L.) leaves, *Phytochemistry* 69 (2008)  
 341 (2008–2015).  
 342 [14] A.V. Ogorodnikova, L.R. Latypova, F.K. Mukhitova, L.S. Mukhtarova, A.N. Grechkin,  
 343 Detection of divinyl ether synthase in Lily-of-the-Valley (*Convallaria majalis*)  
 344 roots, *Phytochemistry* 69 (2008) 2793–2798.

- [15] A.V. Ogorodnikova, F.K. Mukhitova, A.N. Grechkin, Screening of divinyl ether syn- 345  
 thase activity in nonphotosynthetic tissue of asparagales, *Dokl. Biochem. Biophys.* 346  
 449 (2013) 116–118. 347  
 [16] P.J. Proteau, W.H. Gerwick, Divinyl ethers and hydroxy fatty acids from three species 348  
 of *Laminaria* (brown algae) *Lipids* 28 (1993) 783–787. 349  
 [17] Z.D. Jiang, W.H. Gerwick, Novel oxylipins from the temperate red alga *Polysiphonia* 350  
*latissima*: evidence for an arachidonate 9(S)-lipoxygenase, *Lipids* 32 (1997) 351  
 231–235. 352  
 [18] A. Itoh, G.A. Howe, Molecular cloning of a divinyl ether synthase. Identification as a 353  
 CYP74 cytochrome P-450, *J. Biol. Chem.* 276 (2001) 3620–3627. 354  
 [19] M. Stumpe, R. Kandzia, C. Göbel, S. Rosahl, I. Feussner, A pathogen-inducible divinyl 355  
 ether synthase (CYP74D) from elicitor-treated potato suspension cells, *FEBS Lett.* 356  
 507 (2001) 371–376. 357  
 [20] A. Fammartino, F. Cardinale, C. Göbel, L. Mène-Saffrané, J. Fournier, I. Feussner, M.T. 358  
 Esquerré-Tugayé, Characterization of a divinyl ether biosynthetic pathway specifi- 359  
 cally associated with pathogenesis in tobacco, *Plant Physiol.* 143 (2007) 378–388. 360  
 [21] M. Stumpe, J.-G. Carsjens, C. Göbel, I. Feussner, Divinyl ether synthesis in garlic 361  
 bulbs, *J. Exp. Bot.* 59 (2008) 907–915. 362  
 [22] Y.V. Gogolev, S.S. Gorina, N.E. Gogoleva, Y.Y. Toporkova, I.R. Chechetkin, A.N. 363  
 Grechkin, Green leaf divinyl ether synthase: gene detection, molecular cloning 364  
 and identification of a unique CYP74B subfamily member, *Biochim. Biophys. Acta* 365  
 1821 (2012) 287–294. 366  
 [23] G. Granér, M. Hamberg, J. Meijer, Screening of oxylipins for control of oilseed rape 367  
 (*Brassica napus*) fungal pathogens, *Phytochemistry* 63 (2003) 89–95. 368  
 [24] T. Cowley, D. Walters, Local and systemic effects of oxylipins on powdery mildew in- 369  
 fection in barley, *Pest Manag. Sci.* 61 (2005) 572–576. 370  
 [25] I. Prost, S. Dhondt, G. Rothe, J. Vicente, M.J. Rodríguez, N. Kift, F. Carbonne, G. 371  
 Griffiths, M.-T. Esquerré-Tugayé, S. Rosahl, C. Castresana, M. Hamberg, J. 372  
 Fournier, Evaluation of the antimicrobial activities of plant oxylipins supports 373  
 their involvement in defense against pathogens, *Plant Physiol.* 139 (2005) 374  
 1902–1913. 375  
 [26] A. Fammartino, B. Verdager, J. Fournier, G. Tamietti, F. Carbonne, M.-T. Esquerré- 376  
 Tugayé, F. Cardinale, Coordinated transcriptional regulation of the divinyl ether bio- 377  
 synthetic genes in tobacco by signal molecules related to defense, *Plant Physiol.* 378  
*Biochem.* 48 (2010) 225–231. 379  
 [27] V. Balaji, G. Sessa, C.D. Smart, Silencing of host basal defense response-related gene 380  
 expression increases susceptibility of *Nicotiana benthamiana* to *Clavibacter* 381  
*michiganensis* subsp. *michiganensis*, *Phytopathology* 101 (2011) 349–357. 382  
 [28] K. Stránský, J. Tomáš, A. Vitek, An improved method of characterizing fatty acids by 383  
 equivalent chain length values, *J. High Resolut. Chromatogr.* 15 (1992) 730–740. 384  
 [29] Y.Y. Toporkova, Y.V. Gogolev, L.S. Mukhtarova, A.N. Grechkin, Determinants 385  
 governing the CYP74 catalysis: conversion of allene oxide synthase into hydroper- 386  
 oxide lyase by site-directed mutagenesis, *FEBS Lett.* 582 (2008) 3423–3428. 387  
 [30] Y.Y. Toporkova, V.S. Ermilova, S.S. Gorina, L.S. Mukhtarova, E.V. Osipova, Y.V. 388  
 Gogolev, A.N. Grechkin, Structure–function relationship in the CYP74 family: con- 389  
 version of divinyl ether synthases into allene oxide synthases by site-directed mu- 390  
 tagenesis, *FEBS Lett.* 587 (2013) 2552–2558. 391

392